Quantum fluctuations and the Lorenz equations

1986 J. Phys. A: Math. Gen. 19 2751

(http://iopscience.iop.org/0305-4470/19/14/014)

J. Phys. A: Math. Gen. 19 (1986) 2751-2764. Printed in Great Britain

Quantum fluctuations and the Lorenz equations

Sarben Sarkar, J S Satchell† and H J Carmichael‡

Centre for Theoretical Studies, Royal Signals and Radar Establishment, Great Malvern, Worcs WR14 3PS, UK

Received 5 August 1985

Abstract. The quantisation of the Lorenz equations is shown to take the form of a set of two complex and one real stochastic differential equations with multiplicative noise. Phase diffusion is the dominant feature for small values of the noise. Quantities such as the probability of the modulus of the variables are unchanged from those in the classical Lorenz equations. Moreover a fractal dimension can be associated with the stochastic process for sufficiently small noise. For large noises there is a radical breakdown of this picture.

1. Introduction

Recently it has become increasingly appreciated that many systems described by a small number of coupled ordinary differential equations show behaviour which is more complicated than that of a fixed point or of a limit cycle. The attracting sets of such flows are called strange. Apart from their peculiar multi-sheeted structure, it is found that neighbouring points on the attractors have exponentially diverging trajectories as time progresses, and this is an essential feature of the chaos in chaotic attractors. The first illustration of such a system was provided by Lorenz [1] in connection with a very approximate description of a problem in fluids related to Rayleigh-Bénard flow. His equations in suitable variables can be written as

$$\dot{x} = \sigma(y - x) \qquad \dot{y} = zx - y \qquad \dot{z} = -xy + b(r - z). \tag{1}$$

Sometime later Haken [2] pointed out that the same Lorenz equations are in fact quite a good representation of a bad cavity laser with very strong pumping. The Lorenz equations are the Maxwell-Bloch [3] equations in this context. These equations have been the focus of intensive study both in the past and currently. Within the context of laser theory the Lorenz equations represent a semiclassical treatment (i.e. the field has been treated classically but the discrete energy level structure of the atoms, truncated to two, has been taken into account). It is then natural to ask what are the effects of intrinsic quantum fluctuations on a system which, with these fluctuations neglected, shows chaos. It must be stated that in an experimental situation there are likely to be other more important sources [4] of noise. However, given a particular system it is not possible to control the intrinsic fluctuations whereas external noise might be

† Also at: Clarendon Laboratory, University of Oxford, Oxford, UK.

‡ Permanent address: Physics Department, University of Arkansas, Fayetteville, AR 72701, USA.

0305-4470/86/142751+14$02.50

controlled with suitable adjustment of parameters. The question of the role of quantum fluctuations has been addressed within the context of Hamiltonian systems. So far little has been done for dissipative differential systems. A fundamental qualitative fact has to be appreciated. Classical morphologies of chaos are fractal, i.e. have structure to arbitrarily small scales. By its very nature, quantum mechanics dictates that phase space volumes smaller than the quantum phase space volume h^n (where n is some suitable integer) cannot be significant. This is a qualitative argument and we need suitable quantitative measures for the fuzziness of the attractors. One straightforward attempt [5] has been recently made which involves truncating the infinite hierarchy of differential time evolution equations for correlation functions (implied by the master equation for the density matrix of the system). Such truncations are invariably difficult to justify and chaos is not a robust property of such systems, i.e. small changes in the truncation procedures can result in qualitative changes in the trajectories of the correlation functions. Owing to the unreliability of the truncation methods we will study the Fokker–Planck equation related to the master equation.

A dissipative system can be modelled by a purely Hamiltonian [6] system where Hamiltonians for the heat baths and reservoirs (the sources of dissipation) are explicitly included. Standard assumptions concerning the Markov nature of the bath correlation and weak coupling of the system of interest to the bath give a master equation for the density matrix. This is an operator equation and is difficult to solve in general without further approximations [7, 8]. Following Wigner [9, 10] it is possible to construct quantum characteristic functions which generate symmetrised Green functions. The master equation implies a corresponding equation for this characteristic function which is in general exceedingly complicated. However, since the number of atoms in the laser is large, a system size expansion is possible. This implies a Fokker–Planck equation for the quasi-probability distribution associated with the characteristic function. This distribution is known as the Wigner function. If the diffusion matrix is positive definite then it is possible to formulate the Fokker–Planck equation as an equivalent Ito stochastic differential equation (SDE) with a deterministic drift part and a multiplicative noise contribution. The Wigner phase space consists of two complex and one real variable corresponding to the field, polarisation and inversion. The expectation value of any product of classical operators with respect to the Wigner function is equal to the associated quantum mechanical expectation value for the symmetrised product of field, polarisation and inversion operators. In the absence of noise, we just recover the standard Lorenz equations.

In general there are no analytic techniques for solving SDE. Schematically, given a stochastic quantity $u(t)$ which obeys a SDE of the form

$$\mathrm{d}u(t) = \alpha(u(t), t)\,\mathrm{d}t + \beta(u(t), t)\,\mathrm{d}W(t) \tag{2}$$

where α and β are arbitrary functions and $W(t)$ is the Wiener process, then taking a monotonic mesh of time values with $t_n = t$ we have approximately

$$u_{i+1} = u_i + \alpha(u_i, t_i)\Delta t_i + \beta(u_i, t_i)\Delta W_i. \tag{3}$$

The notation is as follows:

$$\alpha_i = \alpha(t_i) \qquad \Delta t_i = t_{i+1} - t_i \qquad \Delta W_i = W(t_{i+1}) - W(t_i). \tag{4}$$

This approximation gives the mean and variance of the stochastic process correct to $O(\Delta t)$. It is in principle possible to have higher-order approximations, but the formulae become very complicated even at the next order [11]. We will base our numerical

simulations on the algorithm of equation (3) with the ΔW_i generated by suitable random number generators which are widely available.

It is possible to associate a fractal dimension with self-similar stochastic processes. Recently, definitions of dimension similar to, but different from, the usual fractal dimension [12] have been introduced. These do not involve box counting algorithms for the whole attractor and are easier to use for multidimensional situations. We adopt the dimension proposed by Termonia and Alexandrowicz [13, 14] which is based on the distribution of distances between points in a time series. We find that from small to moderate amounts of noise, phase diffusion seems to be the dominant effect and the dimension of the attractor (estimated to be 2.08 in the absence of noise) increases to 3.02, an increase of about one. This is discussed fully in the next section. When the noise is large, there does not seem to be a unique dimension.

The phase space trajectories for a single representative of the ensemble could be regarded as the output for a particular experiment. In particular, the phase portrait of the imaginary part of the electromagnetic field against the real part shows rapid bursts of radiation with a particular phase, which changes over time. These bursts may be experimentally verifiable. Just as in the case of deterministic chaos [15], it is interesting to calculate both auto- and cross-correlations of the real and imaginary parts of x, y and z. It is important to note that, although the autocorrelation of Re z has a much sharper decay in the large noise case, there are still fairly periodic oscillations with mean frequency only slightly raised from that found in the ordinary Lorenz model. There is no behaviour in the other correlation functions which is not decaying and no evidence for any chaotic time evolution. When the probability distribution for Re x is calculated the characteristic structure found for the deterministic system is essentially smoothed out to give a non-Gaussian decaying probability distribution P. Similar behaviour is found for $P(\mathrm{Re}\, y)$ and $P(\mathrm{Im}\, y)$. However, again the z variable does not seem to follow this pattern. The distribution of z still retains much of the structure found in the purely deterministic case even for quite large values of the noise.

In § 2 the details of the master equation, the resultant approximate Fokker-Planck equation and Ito stochastic differential equation will be given. In § 3 the calculations sketched above will be discussed fully.

2. Stochastic differential equations

The laser medium will be modelled as a homogeneously broadened system of N two-level atoms interacting with a single mode of the radiation field in the cavity. Pauli raising and lowering operators σ_μ^+ and σ_μ^- and inversion operator σ_μ^z are associated with the μth atom. The commutation relations for these operators are

$$[\sigma_\mu^+, \sigma_\nu^-] = 2\sigma_\mu^z \delta_{\mu\nu} \qquad [\sigma_\mu^z, \sigma_\nu^\pm] = \pm\sigma_\mu^\pm \delta_{\mu\nu}. \tag{5}$$

Operators a, a^+ will denote the single-mode raising and lowering operators. The commutation relation is

$$[a, a^+] = 1. \tag{6}$$

Using standard technique [6] reservoirs (responsible for decays in the system as well as for pumping), it is possible to obtain the following Markovian master equation

$$\frac{\mathrm{d}\rho}{\mathrm{d}t} = \frac{1}{\mathrm{i}\hbar}[H, \rho] + ([a\rho, a^+] + [a, \rho a^+]) + L_A\rho. \tag{7}$$

Here

$$H = igh \sum_{\mu=1}^{N} [\exp(-i\boldsymbol{k}\cdot\boldsymbol{x}_\mu)a^+\sigma_\mu^- - \exp(i\boldsymbol{k}\cdot\boldsymbol{x}_\mu)a\sigma_\mu^+] \tag{8}$$

$$L_A\rho = \tfrac{1}{2}\sum_{\mu=1}^{N} \{\gamma_\uparrow([\sigma_\mu^+, \rho\sigma_\mu^-] + [\sigma_\mu^+\rho, \sigma_\mu^-]) + \gamma_\downarrow([\sigma_\mu^-, \rho\sigma_\mu^+] + [\sigma_\mu^-\rho, \sigma_\mu^+])$$
$$+ \gamma_0([\sigma_\mu^z, \rho\sigma_\mu^z] + [\sigma_\mu^z\rho, \sigma_\mu^z])\} \tag{9}$$

where $\boldsymbol{k}$ is the wavevector of the field mode, $\boldsymbol{x}_\mu$ is the position vector of the μth atom, κ is the cavity damping rate, $\gamma_\downarrow$ is the Einstein A coefficient, $\gamma_\uparrow$ is the pumping rate from the lower to the upper level of the atoms, γ_0 is a rate for the collision-induced phase decay of the atoms and $g(=(2\pi\omega\bar{\mu}^2/hV)^{1/2})$ is the atom–field coupling constant, where $\bar{\mu}$ is the absolute value of the atomic dipole moment.

Clearly there is net pumping only if $\gamma_\uparrow > \gamma_\downarrow$.

We introduce the operators

$$\chi_\mu(\xi, \xi^*, \eta) = \exp i[\xi^*\sigma_\mu^+ \exp(i\boldsymbol{k}\cdot\boldsymbol{x}_\mu) + \eta\sigma_\mu^z + \xi\sigma_\mu^- \exp(-i\boldsymbol{k}\cdot\boldsymbol{x}_\mu)] \tag{10}$$

$$\chi = \prod_{\mu=1}^{N} \chi_\mu \tag{11}$$

$$\bar{\chi} = \exp i(\zeta^* a^+ + \zeta a) \tag{12}$$

$$\chi = \chi\bar{\chi} \tag{13}$$

and characteristic function

$$C_N(\xi, \xi^*, \eta, \zeta, \zeta^*) = \mathrm{Tr}(\hat{\chi}_\zeta). \tag{14}$$

The generalised Wigner distribution P is then defined by

$$C_N(\xi, \xi^*, \eta, \eta^*) = \int \cdots \int d\bar{\zeta}_x\, d\bar{\zeta}_y\, d\bar{\xi}_x\, d\bar{\xi}_y\, d\bar{\eta}\, P(\bar{\xi}, \bar{\xi}^*, \bar{\eta}, \bar{\zeta}, \bar{\zeta}^*)$$
$$\times \exp i(\bar{\zeta}\zeta + \bar{\zeta}^*\zeta^* + \bar{\xi}^*\bar{\xi} + \bar{\xi}\xi + \bar{\eta}\eta) \tag{15}$$

and

$$\bar{\zeta} = \bar{\zeta}_x + i\bar{\zeta}_y \qquad \bar{\xi} = \bar{\xi}_x + i\bar{\xi}_y. \tag{16}$$

The master equation implies an equation for C and, for this to be satisfied, it is sufficient that P satisfies an equation which, to second order in the derivatives, is a Fokker–Planck equation. It is useful to introduce scaled variables

$$\bar{m} = (2/N)\bar{\eta} \tag{17}$$

$$\bar{v} = \bar{v}_1 + i\bar{v}_2 = -\frac{2}{N}\left(\frac{\gamma_\perp}{\gamma_\downarrow}\right)^{1/2}\bar{\xi} \tag{18}$$

$$\bar{x} = \bar{x}_1 + i\bar{x}_2 = n_0^{-1/2}\bar{\zeta} \tag{19}$$

where

$$\gamma_\perp = 2\gamma_0 + \tfrac{1}{2}\gamma_\downarrow \tag{20}$$

and n_0 is the saturation photon number given by

$$n_0 = \gamma_\downarrow N/8\kappa C \tag{21}$$

where $C = g^2N/\kappa\gamma_\downarrow$.

In terms of $\{\bar{v}_1, \bar{v}_2, \bar{x}_1, \bar{x}_2, \bar{m}\}$ the equation for P is

$$\frac{\partial P}{\partial t} = \left\{ \gamma_\perp \frac{\partial}{\partial \bar{v}_1}(\bar{v}_1 + \bar{m}x_1) + \gamma_\perp \frac{\partial}{\partial \bar{v}_2}(\bar{v}_2 + \bar{m}x_2) + \kappa\left(\frac{\partial}{\partial \bar{x}_1}(\bar{x}_1 + 2C\bar{v}_1) + \frac{\partial}{\partial \bar{x}_2}(\bar{x}_2 + 2C\bar{v}_2)\right)\right.$$

$$+ \gamma_\parallel \frac{\partial}{\partial \bar{m}}(\bar{m} - \hat{\sigma} - \bar{v}_1\bar{x}_1 - \bar{v}_2\bar{x}_2)$$

$$+ \gamma_\perp^2 (2C\kappa n_0)^{-1}\left[\frac{1}{4}\left(\frac{\partial^2}{\partial \bar{v}_1^2} + \frac{\partial^2}{\partial \bar{v}_2^2}\right) + f^2 \frac{\partial^2}{\partial m^2}(1 - \sigma\bar{m})\right.$$

$$\left.\left. - \hat{\sigma} f^2 \frac{\partial}{\partial \bar{m}}\left(\frac{\partial}{\partial \bar{v}_1}\bar{v}_1 + \frac{\partial}{\partial \bar{v}_2}\bar{v}_2\right)\right] + \frac{\kappa}{4n_0}\left(\frac{\partial^2}{\partial \bar{x}_1^2} + \frac{\partial^2}{\partial \bar{x}_2^2}\right)\right\} P. \tag{22}$$

Here

$$\hat{\sigma} = (\gamma_\uparrow - \gamma_\downarrow)/(\gamma_\uparrow + \gamma_\downarrow) \tag{23}$$

$$\gamma_\parallel = \gamma_\uparrow + \gamma_\downarrow \tag{24}$$

$$f = \gamma_\parallel / 2\gamma_\perp . \tag{25}$$

The diffusion matrix D in the basis $(\bar{x}_1, \bar{x}_2, \bar{v}_1, \bar{v}_2, \bar{m})$ has the form

$$D = \begin{pmatrix} \frac{\kappa}{2n_0} & 0 & & & \\ 0 & \frac{\kappa}{2n_0} & & & \\ & & \frac{\gamma_\perp^2}{4\kappa C n_0} & 0 & \frac{-\gamma_\perp^2 \hat{\sigma} f^2}{2\kappa C n_0}\bar{v}_1 \\ & & 0 & \frac{\gamma_\perp^2}{4\kappa C n_0} & \frac{-\gamma_\perp^2 \hat{\sigma} f^2}{2\kappa C n_0}\bar{v}_2 \\ & & \frac{-\gamma_\perp^2 \hat{\sigma} f^2 \bar{v}_1}{2\kappa C n_0} & \frac{-\gamma_\perp^2 \hat{\sigma} f^2 \bar{v}_2}{2\kappa C n_0} & \frac{\gamma_\perp^2 f^2 (1 - \hat{\sigma}\bar{m})}{\kappa C n_0} \end{pmatrix}. \tag{26}$$

Since the D matrix separates into a 2×2 and a 3×3 block, we will concentrate on the latter block and denote it by $D^{(3)}$:

$$D^{(3)} = \frac{\gamma_\perp^2}{4\kappa C n_0} dd^T \tag{27}$$

where a suitable d is given by

$$d = \begin{pmatrix} 1 & 0 & 0 \\ 0 & 1 & 0 \\ -2\hat{\sigma} f^2 \bar{v}_1 & -2\hat{\sigma} f^2 \bar{v}_2 & 2f(1 - \hat{\sigma}\bar{m} - \hat{\sigma}^2 f^2 (\bar{v}_1^2 + \bar{v}_2^2))^{1/2} \end{pmatrix}. \tag{28}$$

d is, of course, unique only up to orthogonal transformations. Using the given form of d it is possible to write down the Ito-Langevin equations corresponding to the Fokker-Planck equation. These are

$$\mathrm{d}\bar{x} = -k(\bar{x} + 2C\bar{v})\,\mathrm{d}t + (\kappa/2n_0)^{1/2}\,\mathrm{d}W_x \tag{29}$$

$$\mathrm{d}\bar{v} = -\gamma_\perp(\bar{v} + \bar{m}\bar{x})\,\mathrm{d}t + [\gamma_\perp/2(\kappa C n_0)^{1/2}]\,\mathrm{d}W_y \tag{30}$$

$$\mathrm{d}\bar{m} = -\gamma_{\parallel}(\bar{m} - \hat{\sigma} - \tfrac{1}{2}(\bar{v}^*\bar{x} + \bar{v}\bar{x}^*))\,\mathrm{d}t + \frac{\gamma_{\perp} f}{(\kappa C n_0)^{1/2}}$$

$$\times\left(-\frac{\hat{\sigma} f}{2}(\bar{v}^*\,\mathrm{d}W_y + \bar{v}\,\mathrm{d}W_y^*) + (1 - \hat{\sigma}\bar{m} - \hat{\sigma}^2 f^2 \bar{v}\bar{v}^*)^{1/2}\,\mathrm{d}W_z\right) \tag{31}$$

$$\mathrm{d}W_x = \mathrm{d}W_1 + \mathrm{i}\,\mathrm{d}W_2 \qquad \mathrm{d}W_y = \mathrm{d}W_3 + \mathrm{i}\,\mathrm{d}W_4 \qquad \mathrm{d}W_z = \mathrm{d}W_5. \tag{32}$$

W_i $(i = 1\text{-}5)$ are independent Wiener processes. In order to make the equations reduce, in the absence of noise, to the form of the Lorenz equations given in equation (1), it is necessary to introduce the rescaled variables

$$x = -(b/2)^{1/2}\bar{x} \qquad y = (2b)^{1/2}C\bar{v} \qquad z = 2C\bar{m} \tag{33}$$

and

$$\tau = \gamma_{\perp} t$$

with the well known Lorenz parameters defined as

$$b = \gamma_{\parallel}/\gamma_{\perp} \qquad \sigma = x/\gamma_{\perp} \qquad r = 2c\hat{\sigma}. \tag{34}$$

Then the stochastic generalisation of the Lorenz equations is

$$\mathrm{d}x = \sigma(y - x)\,\mathrm{d}\tau - (2/C)^{1/2}\sigma\varepsilon\,\mathrm{d}W_x \tag{35}$$

$$\mathrm{d}y = (xz - y)\,\mathrm{d}\tau + 2\varepsilon\,\mathrm{d}W_y \tag{36}$$

$$\mathrm{d}z = -b(z - r)\,\mathrm{d}\tau - (xy^* + x^*y)\,\mathrm{d}\tau - (br\varepsilon/4C^2)(y^*\,\mathrm{d}W_y + y\,\mathrm{d}W_y^*)$$
$$+ 2^{3/2}\varepsilon b^{1/2}[1 - rz/4C^2 - (r^2 b/32C^4)yy^*]^{1/2}\,\mathrm{d}W_z. \tag{37}$$

Apart from x and y being complex, a new feature is the introduction of two constants ε and C. In terms of the laser parameters ε is defined as

$$\varepsilon = (Cb/8\sigma n_0)^{1/2}. \tag{38}$$

These equations are only consistent if

$$1 - rz/4C^2 - (r^2 b/32C^4)yy^* \geqslant 0. \tag{39}$$

This condition is equivalent to the requirement of a positive definite diffusion matrix. For moderately large C (such as $C = 50$) the above positivity holds, and these are the cases that are being considered. Unless otherwise stated our calculations in the chaotic regime will assume $r = 28$, $\sigma = 10$, $b = \frac{8}{3}$ and $C = 50$.

3. Statistical and fractal properties

We will first recall a few properties of the statistical properties [15] of the standard Lorenz equations in the chaotic regime. The quantities studied are $P(x)$, the probability distribution of x, i.e. the projection of the attractor on the x axis, and normalised intensity moments $m(r)$ given by

$$m(r) = \int P(x^2)x^{2r}\,\mathrm{d}x^2\left(\int P(x^2)x^2\,\mathrm{d}x^2\right)^{-r}. \tag{40}$$

Moments for $r = 2, 3, 4$ and 5 show a non-Gaussian property. The lowest moments lie above those of a negative exponential distribution, but the higher moments fall substantially below (reflecting the finite support of the strange attractor). The non-Gaussian nature of the statistics is also evident from the symmetric triple-peaked structure of $P(x)$ with cutoffs at finite values of x. Correlation functions of the variables are calculated using the definition

$$\langle A(t)B(0)\rangle = \lim_{T\to\infty} \frac{1}{T}\int_0^T \mathrm{d}\xi\, A(t+\xi)B(\xi) \tag{41}$$

where A and B may represent any of the Lorenz variables. In particular, as is common in quantum optics, $g^{(1)}$ and $g^{(2)}$ are computed. These are defined to be

$$g^{(1)}(t) = \frac{\langle x(t)x(0)\rangle}{\langle (x(0))^2\rangle} \tag{42}$$

$$g^{(2)}(t) = \frac{\langle x^2(t)x^2(0)\rangle}{\langle (x(0))^2\rangle^2}. \tag{43}$$

$g^{(1)}$ shows little evidence of periodic behaviour and decays fast. $g^{(2)}$ initially decays fast but then falls off more slowly to the asymptotic value of unity and also exhibits a regular oscillation. This extra structure in $g^{(2)}$ is again indicative of non-Gaussian statistics.

In the lasing region ($r < \sigma(\sigma+b+3)(\sigma-b-1)^{-1}$) it is well known that the phase of the field ($\arg X$) diffuses randomly when the effect of the noise is included. This is also true in the chaotic region, as we can see from the X projection of a sample trajectory shown in figure 1, where the noise ε is 0.1. Interestingly the diffusion seems to be most rapid for small values of $|x|$; the phase of any one burst of output is relatively constant but the phase of successive bursts may differ appreciably. This can be seen most clearly from figure 2, an expanded view of the centre of figure 1. As the intensity between the bursts is typically quite low (<0.1% of the peak intensity) it appears that the system loses its phase memory and is being overridden by the noise.

If the largest effect of the noise in our model is to change the phase of the field (X) and polarisation (Y) variables, we would expect the probability distributions for $|X|$ and $|Y|$ to be less affected than those for $\mathrm{Re}(X)$ and $\mathrm{Re}(Y)$. Figures 3-11 show the unnormalised probability distributions for $|X|$, $|Y|$ and Z for $\varepsilon = 0$, 0.1 and 1.0 respectively. For comparison the unnormalised distributions for $\mathrm{Re}(X)$ and $\mathrm{Re}(Y)$ are shown in figures 12 and 13 for $\varepsilon = 0.1$. It is obvious that the distributions for the moduli are largely unchanged except for the largest noise case where the peak at the origin has been replaced by a dip.

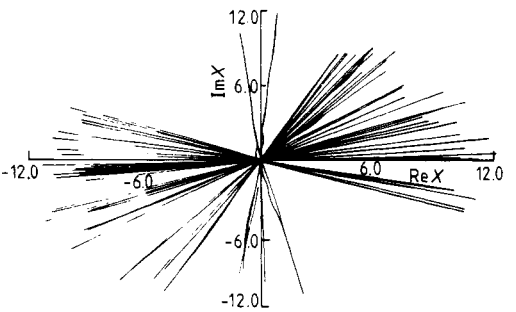

Figure 1. X projection of a sample trajectory with $\varepsilon = 0.1$.

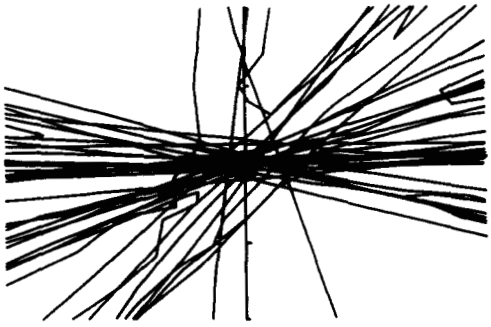

Figure 2. An expanded version of the centre of figure 1.

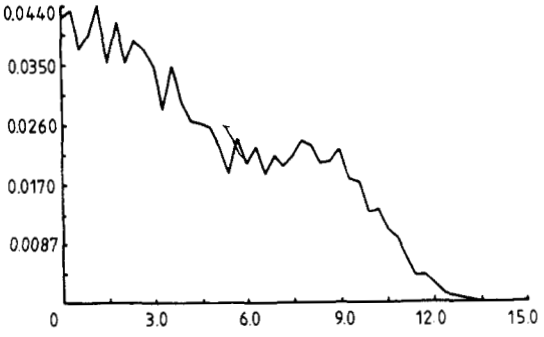

Figure 3. Probability distribution for $|X|$ with $\varepsilon = 0$.

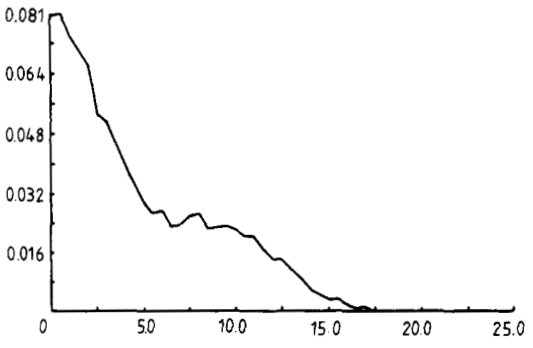

Figure 4. Probability distribution for $|Y|$ with $\varepsilon = 0$.

This is further borne out by examining the normalised moments of the intensity distribution. These are given in table 1 and it is apparent that for $\varepsilon < 1$ the moments are essentially unchanged, indicating that the effect of the noise has largely been confined to altering the phase of the field rather than its intensity. We note that for the largest noise the moments are considerably reduced. This is consistent with the distribution for $|X|$ being peaked away from the origin when $\varepsilon = 1$ (see figure 9) and hence we would also expect a more peaked distribution for $|X|^2$. In fact, in the absence of noise the point ($x = y = 0$ and $z = r$) has a two-dimensional stable manifold.

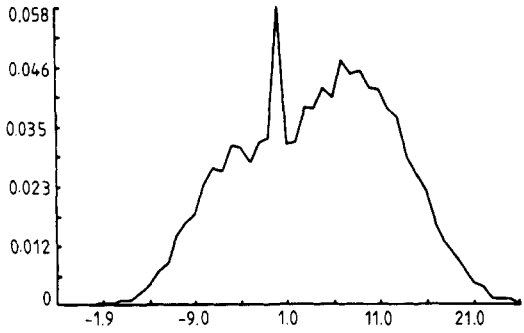

Figure 5. Probability distribution for z with $\varepsilon = 0$.

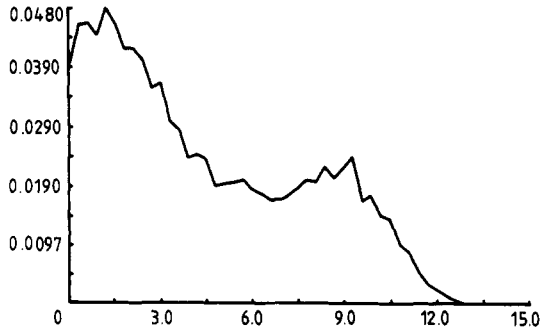

Figure 6. Probability distribution for $|X|$ with $\varepsilon = 0.1$.

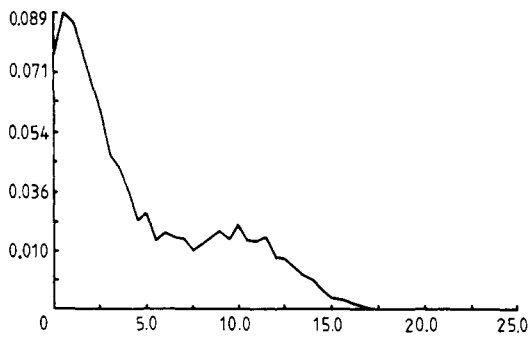

Figure 7. Probability distribution for $|Y|$ with $\varepsilon = 0.1$.

Moreover the velocity of motion near this point is very slow. This gives a peak at $|X| = 0$ for the distribution for $|X|$. In the presence of noise it would be expected that the trajectories would receive impulses transverse to the manifold and along the unstable manifold. This would shift the peak of the distribution for $|X|$ away from the origin.

The effect of the noise on the autocorrelations is small except for the largest values used ($\varepsilon = 1$) where we find that the correlations decay a little more rapidly. This is apparently because the phase of the field diffuses slowly compared with the decay times of the autocorrelations for X and Y and the noise amplitudes we have used do not appreciably alter the moduli of the system. This is consistent with the findings of Zippelius and Lucke [16] who studied the standard Lorenz model with constant

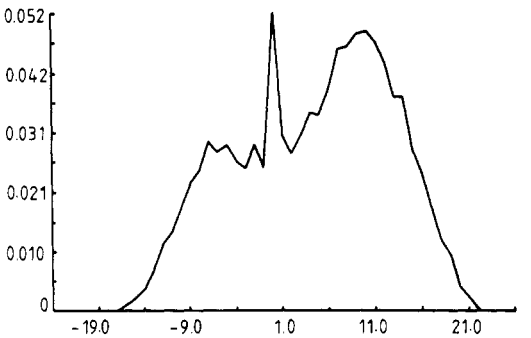

Figure 8. Probability distribution for z with $\varepsilon = 0.1$.

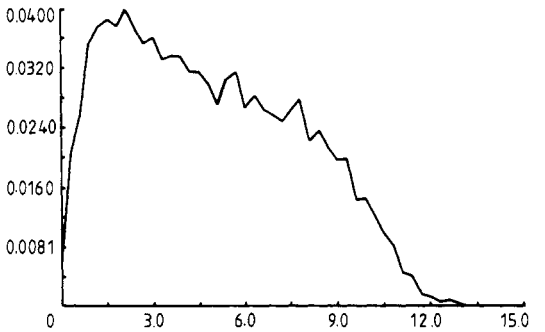

Figure 9. Probability distribution for $|X|$ with $\varepsilon = 1.0$.

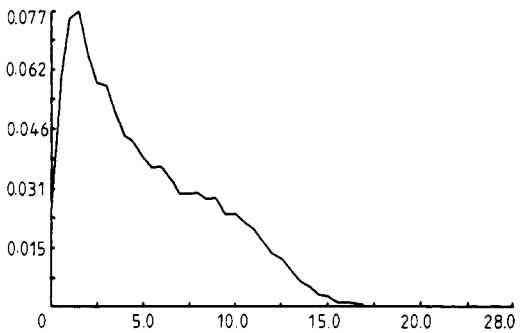

Figure 10. Probability distribution for $|Y|$ with $\varepsilon = 1.0$.

amplitude additive noise. They found that there was little change in the autocorrelations for noise amplitudes below 1.

Figures 14 and 15 show $\langle \mathrm{Re}\, x(t)\ \mathrm{Re}\, x(t+\tau)\rangle$ for $\varepsilon = 0$ and $\varepsilon = 1.0$, figures 16 and 17 show the same for Y and figures 18 and 19 show $\langle z(t)z(t+\tau)\rangle$. Notice that the strong oscillations in figure 18 decay more rapidly in figure 19.

Various exponents, collectively known as fractal dimensions [12], have been introduced in the study of deterministic chaos to measure the non-Euclidean topology of strange attractors. Whereas the original Lorenz equations involve three variables, the corresponding SDE have two complex and one real. We have seen already that the trajectories explore this larger space and consequently the fractal dimension of the

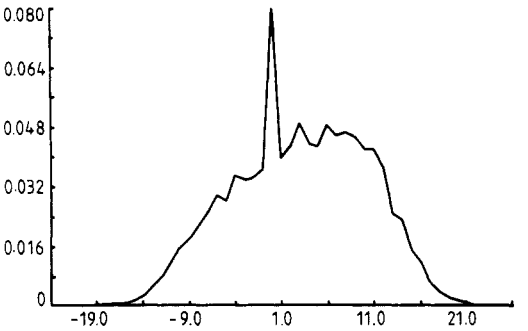

Figure 11. Probability distribution for z with $\varepsilon = 1.0$.

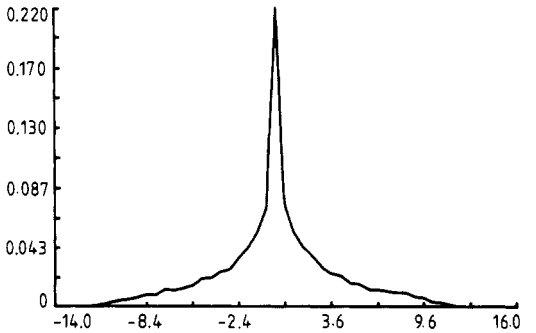

Figure 12. Probability distribution for Re x with $\varepsilon = 0.1$.

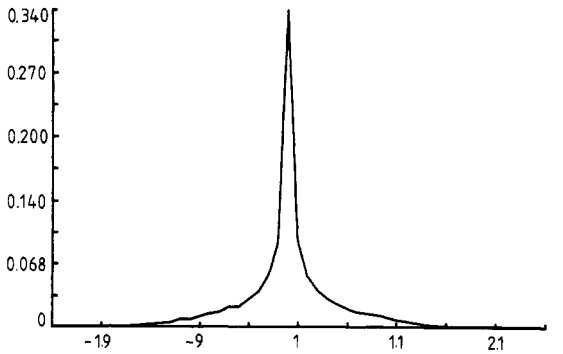

Figure 13. Probability distribution for Re y with $\varepsilon = 0.1$.

Table 1. Normalised intensity moments.

Epsilon	M2	M3	M4	M5
0	2.28	6.6	21.5	75.4
0.01	2.32	6.8	22.1	77.4
0.03	2.31	6.7	21.7	76.5
0.1	2.33	6.8	22.1	77.4
1.0	1.91	4.71	13.35	41.8

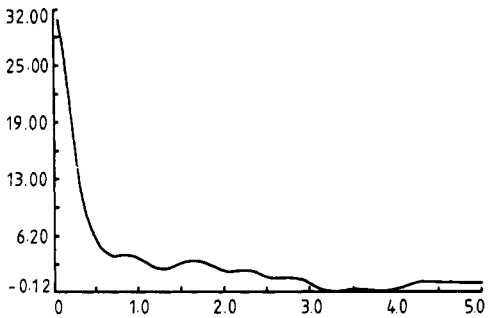

Figure 14. $\langle \mathrm{Re}\, x(t)\, \mathrm{Re}\, x(t+\tau)\rangle$ for $\varepsilon = 0$.

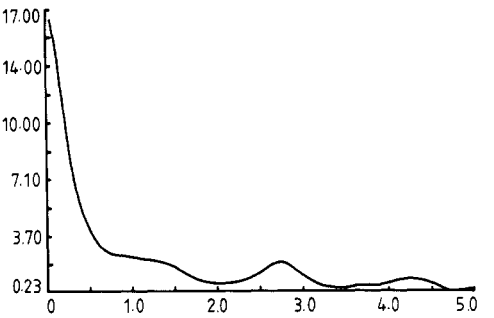

Figure 15. $\langle \mathrm{Re}\, x(t)\, \mathrm{Re}\, x(t+\tau)\rangle$ for $\varepsilon = 1.0$.

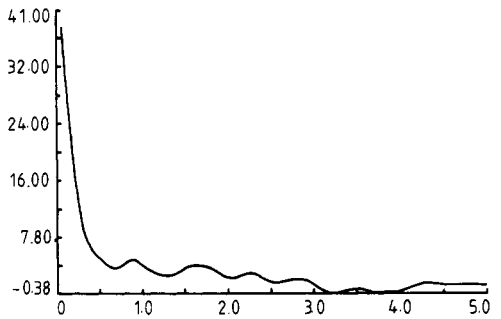

Figure 16. $\langle \mathrm{Re}\, y(t)\, \mathrm{Re}\, y(t+\tau)\rangle$ for $\varepsilon = 0$.

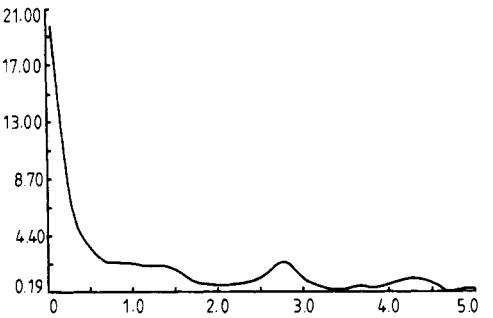

Figure 17. $\langle \mathrm{Re}\, y(t)\, \mathrm{Re}\, y(t+\tau)\rangle$ for $\varepsilon = 1.0$.

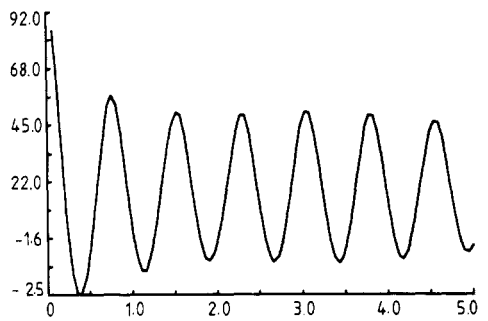

Figure 18. $\langle z(t)z(t+\tau)\rangle$ for $\varepsilon = 0$.

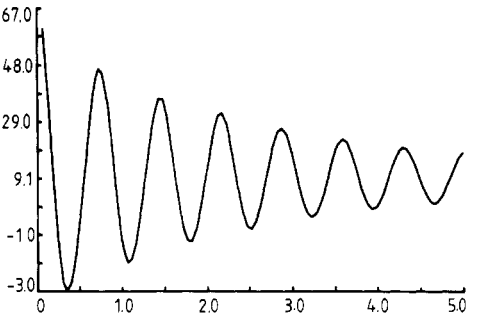

Figure 19. $\langle z(t)z(t+\tau)\rangle$ for $\varepsilon = 1.0$.

stochastic process would be expected to be greater than that found for the deterministic case. That is what is found. A well known dimension used frequently is the capacity D_F. If the strange attractor is embedded in a suitable d-dimensional space and if $N(\varepsilon)$ is the number of d-dimensional spheres of radius ε needed to cover the attractor, then

$$N(\varepsilon) \sim \varepsilon^{-D_F} \qquad \text{as } \varepsilon \to 0. \tag{44}$$

However when d becomes large the algorithms based on this definition become computationally intractable. A dimension $D_{F'}$ has recently been proposed [13, 14]

which is comparatively easy to calculate even for high d. If the attractor is covered by N spheres containing just n points of the time series, it has been argued that

$$n \sim (\bar{R}(n))^{D_{F'}} \tag{45}$$

where $(\bar{R}(n))^d$ is the average volume of a box containing n points. Points on the time series are chosen at random and the distances to all other points in the time series can be calculated. This gives enough information to calculate $\bar{R}(n)$ and hence $D_{F'}$. It is necessary to have a sufficiently long time series since, if it is too short, the distances can begin to become comparable with the total size of the attractor (i.e. the outer scale of the fractal) for the larger values of n. This tends to reduce the values of $D_{F'}$ obtained from the method unless R and n are suitably restricted. The dimensions given below have all been obtained from the small-n region ($n \leqslant 500$) where outer scale effects should be negligible. For a stochastic process such calculations are meaningful if $D_{F'}$ is independent of different realisations of the noise [12]. For large values of the noise ($\varepsilon \sim 0.3$) we have checked that the same values were obtained for different members of an ensemble of 10^4 point time series and for successive 10^4 point sections of a longer time series. This provides a weak first check on the ergodicity of this stochastic fractal process.

For the best accuracy we considered the longest time series that was practicable for us (using a Cray computer). Time series consisting of 5×10^5 points spaced at intervals of 0.2 of a Lorenz time were used (i.e. 10^5 time units in each set). For $\varepsilon = 0$, $\bar{R}(n)$ was obtained from averaging over 512 randomly chosen points. This gave $D_{F'} \sim 2.16$. Similarly, for $\varepsilon = 0.1$, with an average over 640 points, $D_{F'} \sim 3.11$ (see table 2). Of course 10^5 time units allows the phase to have diffused freely around 2π many times. This has been checked by examining projections of sample sections of the trajectories. In the above cases a unique fractal dimension was compatible with the data sets. No evidence for an inner scale was seen. It is always possible that for a longer time series evidence for an inner scale might appear. The larger the noise, the larger will be the inner scale. Hence by examining a case such as $\varepsilon = 0.3$ it may be possible to find the effects of an inner scale with a time series of 5×10^5 points. This is indeed the case. In table 3 $D_{F'}$ is given as a function of n. There is a steady increase of $D_{F'}$ as n decreases. It could well be that for even longer time series there could be evidence for D tending to 5 which would correspond to a fivefold product of independent Wiener processes. These findings are reinforced for larger noise cases. Hence the process is not self-similar and we cannot rigorously use the concept of fractal dimension in these cases. However it is still informative to note that, although the small scale structure has been modified, the larger scale clustering has been altered from the intermediate noise ($\varepsilon \leqslant 0.1$) cases. It appears therefore that, although the attractor may be locally smeared out, some of its structure still survives. Moreover

Table 2. Fractal dimensions (at scales beyond inner scale).

Epsilon	$D_{F'}$	+/− standard error of the mean
0	2.16	0.03
0.01	3.07	0.04
0.03	3.03	0.04
0.1	3.11	0.02
1.0	3.48	0.02

Table 3. Inner scale effects for $\varepsilon = 0.3$.

Range of n	$D_{F'}$
[1, 10]	3.7
[10, 20]	3.5
[20, 30]	3.38
[50, 60]	3.31
[100, 110]	3.23
[200, 210]	3.18
[490, 500]	3.16

this structure seems to be dominated by phase diffusion and this is compatible with the increase of the fractal dimension by about one from the deterministic situation (since the phases of X and Y are closely related).

After this work was completed we came across the paper of Graham [17] in which the Wigner representation was also used. However, apart from this similarity, the approaches are quite different, Graham concentrating on approximate analytic techniques to obtain information on the structure of the attractor in the limit of small noise.

Acknowledgments

HJC thanks RSRE Malvern for its hospitality while he was a Visiting Research Fellow. JSS acknowledges the funding of RSRE of his Research Associateship at the Clarendon Laboratory, Oxford. One of us (SS) thanks J N Elgin for discussions.

References

[1] Lorenz E N 1963 *J. Atmos. Sci.* **20** 130
[2] Haken H 1975 *Phys. Lett.* **53A** 77
[3] Bloch F 1964 *Phys. Rev.* **70** 460
Feynman R P, Vernon F L and Hellwarth R W 1957 *J. Appl. Phys.* **28** 49
Lamb W E Jr 1964 *Phys. Rev.* **134** A1429
Haken H and Sauermann H 1963 *Z. Phys.* **173** 261
[4] Schenzle A and Brand H 1978 *Opt. Commun.* **27** 485
[5] Elgin J N and Sarkar S 1984 *Phys. Rev. Lett.* **52** 1215; **53** 1507
Graham R 1984 *Phys. Rev. Lett.* **53** 1506
[6] Haken H 1970 *Laser Theory. Encyclopaedia of Physics* **XXV/2c** (Berlin: Springer)
[7] Drummond P D and Walls D F 1981 *Phys. Rev.* A **23** 2563
[8] van Kampen N G 1976 *Phys. Rep.* **24C** 171
[9] Wigner E P 1932 *Phys. Rev.* **40** 749
[10] Lugiato L A, Casagrande F and Pizzuto L 1982 *Phys. Rev.* A **26** 3483
[11] Satchell J S and Sarkar S 1986 *J. Phys. A: Math. Gen.* **19** 2737-49
[12] Mandelbrot B B 1982 *The Fractal Geometry of Nature* (San Francisco: Freeman)
[13] Termonia Y and Alexandrowicz Z 1983 *Phys. Rev. Lett.* **51** 1265
[14] Grassberger P and Procaccia I 1983 *Phys. Rev. Lett.* **50** 346
[15] Broomhead D S, Elgin J N, Jakeman E, Sarkar S, Hawkins S C and Drazin P 1984 *Opt. Commun.* **50** 56
[16] Zippelius A and Lücke M 1981 *J. Stat. Phys.* **24** 345
[17] Graham R 1984 *Phys. Rev. Lett.* **53** 2020